

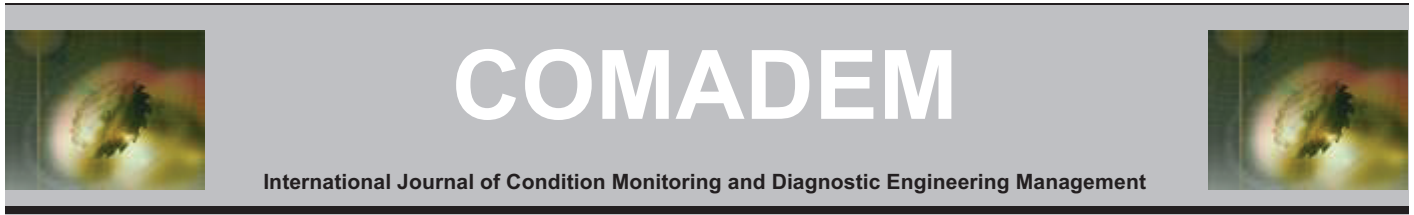
AHMED, N., ASIM, T., MISHRA, R. and NSOM, B. 2019. Flow visualization within a ventricular inhaler device using open source CFD for performance enhancement. *International journal of condition monitoring and diagnostic engineering management* [online], 22(2), pages 21-26. Available from: <https://apscience.org/comadem/index.php/comadem/article/view/142>

Flow visualization within a ventricular inhaler device using open source CFD for performance enhancement.

AHMED, N., ASIM, T., MISHRA, R. and NSOM, B.

2019





Flow visualization within a Ventricular Inhaler Device using Open Source CFD for Performance Enhancement

Noukhez Ahmed ^a, Taimoor Asim ^{b*}, Rakesh Mishra ^c, and Blaise Nsom ^d

^a Faculty of Science and Engineering, University of Wolverhampton, Wulfruna Street, Wolverhampton, UK WV1 1LY

^b School of Engineering, Robert Gordon University, Garthdee Road, Aberdeen, UK AB10 7GJ

^c School of Computing and Engineering, University of Huddersfield, Queensgate, Huddersfield, UK HD1 3DH

^d Université de Bretagne Occidentale, IUT de Brest, IRDL UMR CNRS 6027, France

* Corresponding author. Tel.: +44-1224-262457; email: t.asim@rgu.ac.uk

ABSTRACT

A Ventricular Inhaler Device (VID) is used as a quick-relief medication for treating wheezing and shortness of breath. VID uses Albuterol (a bronchodilator) to relax muscles and open airways. The flow distribution of Albuterol within the VID is the primary parameter that dictates the performance of the device. Poorly designed VIDs can cause accumulation of Albuterol in outlet section of the device, causing flow blockages, which lead to inefficient performance of the device and inappropriate drug delivery. In the present study, Computational Fluid Dynamics (CFD) based advanced techniques have been used in order to visualize the complex flow behavior within a conventional VID, with a purpose to enhance the performance of the device. It has been observed that the pressure coefficient within the injector and outlet duct remains constant, while it decreases in the cyclone separator. Thus, the inlet flow velocity has been seen to have dominating effect on the performance of the VID compared to the rotational velocity of the blades. It has been further noticed that as the flow rate of the drug increases, the efficiency of VID also decreases to a minimum value, after which it remains constant. Moreover, lower rotational speeds of the blades increase the efficiency of the device at higher drug flow rates.

Keywords: Computational Fluid Dynamics (CFD), Ventricular Inhaler Device (VID), pressure coefficient, Reynolds Averages Navier-Stokes (RANS).

1. Introduction

Rapid development in pulmonary drug delivery by inhalation aerosols in the past decade has led to novel invention of aerosol delivery devices and new formulation technologies. These devices have the capability of producing particles of defined characteristics for improved delivery. Extensive research in particle technology has advanced the ventricular inhaler device (VID) formulation by control of drug particle density, particle morphology, particle size, size distribution, particle injection process and system. VID is high advanced pressure Metered Dose Inhaler (pMDI). Additionally, spacers are often used between the inhaler outlet duct and the mouth cavity, which helps in mixing the concentrated dose with air to make it less dense. This helps those patients, who have severe problems with breathing. The key components of the VID device include propellants, formulation, metering dose, metering valve, actuator and cyclone separator comprises of small impeller, all play important roles in the formation of the spray, and in determining drug delivery to the lungs. There is large number of inventions in dry powder inhalers and VIDs, but not much concerns with the inhaler performance at a fundamental level.

The design of a VID is vital to control the size range of drug particles emitted from the device. The drugs used inside the VID are Salbutamol, which is indicated for the treatment or prevention of bronchospasm in patients 4 years of age and older with

reversible obstructive airway disease. It helps in treating various conditions including Exercise-Induced Bronchospasm Prevention, Asthma Attack, Bronchospasm and Chronic Obstructive Lung Disease. VID is designed to be used without the spacer. After the injection region within the VID, a small mixture region known as cyclone separator is created, which consists of an impeller (having three blades) and two air inlet ducts. The combination of air mixture with salbutamol helps the dosage to be fully mixed up. Thereafter the mixed dose is then ejected by the inhaler into patients' mouth cavity. At present, there is little published literature that demonstrates how the design of inhaler affects the pressurized metered dose dispersion performance. Computational Fluid Dynamics (CFD) has found wide application in the study of pharmaceutical unit operations for drug delivery from the inhalers to the lungs. The dispersion and deposition of pharmaceutical aerosols in turbulent airflow is an important consideration when numerically investigating inhaler performance.

Dumbar et al. [1-2] have carried out the first numerical simulations on pMDIs in investigating transport of the droplet and its formation during the actuation of the inhaler and thereafter, experimental investigations have been conducted to benchmark his results using laser diagnostic techniques. However, due to computationally intensive nature of the numerical simulations has prevented the sensitivity tests and hence the results have considered as preliminary. Versteeg et al.

[3] have carried out numerical simulation using steady state airflow and aerosol plume to predict the behavior of flow within two pMDIs; experimental pMDIs and AstraZeneca Pulmicort pMDI. It has been found that the flow within both the inhalers is highly complex but similar. Multiple regions of recirculation within pMDI have been found with high levels of turbulence. Kleinstreuer et al. [4] have carried out investigation on the airflow, droplet transport and its deposition within pMDI and human upper airway model. The effect of spacer used between the pMDI and upper airway and nozzle diameter has been investigated. Chlorofluorocarbon (CFC) and hydrofluoroalkane-134a (HFA) propellant aerosols have been numerically simulated using CFD solver to determine the effect of propellant properties and their deposition. The flow obtained within the inhaler body is highly complex with vortices generation at a steady flowrate of 30l/min. The results obtained for both propellant aerosols are in good agreement with vivo and vitro studies conducted by Leach et al. [5] and Cheng et al. [6] respectively. Minor inconsistencies have been obtained due to assumptions considered in numerical simulations and physical processes including droplet coalescence, which is assumed negligible. Furthermore, it has been observed that better deposition performance has been found in HFA in comparison to CFC. This is due to differences in nozzle diameters considered.

Kleinstreuer et al. [4] also considered the spacer used to quantify its effects on deposition rates for pMDIs with both propellant aerosols. The insertion of spacer between the pMDI and human upper airway model has shown sudden expansion in the volume with reduced flow velocity and higher droplet residence time and evaporation. The sudden reduction in droplet speed and size has reduced deposition in the oral cavity and hence the drug delivery to the lungs has highly increased. The performance of both the propellants CFC and HFA has improved using spacer with the pMDI. Leach and Colice [7] has carried out vivo by pilot study to assess lung deposition of HFA and CFC from a pMDI with and without add-on spacers and using varying breathhold times. The results carried out by Leach and Colice study are compared with Kleinstreuer et al. study. It has been observed that higher proportions of deposition are found in spacer in comparison to numerical simulations. The discrepancies obtained within both studies are due to change in nozzle diameters considered or formulation differences between vivo pMDIs of Leach and Colice and Kleinstreuer et al numerical simulations. Furthermore, variations in the droplet size and velocities considered have significant impact on the deposition as well. However, the trend obtained depicts decreased oropharyngeal deposition with the use of spacer [4, 7]. Oliveria et al. [8] have carried out investigation on the development of a new Volumatic spacer design for better deposition performance. It has been found that design change to the spacer and valve used could reduce large areas of recirculation within the spacer. An optimized design of the spacer has been made by combining the best-performing body and valve geometries by considering a series of different combination of prototypes. It has been found that reduced recirculation and turbulence kinetic energy within pMDI reduces the droplet deposition inside the device and results better drug delivery to the patient lungs.

Farina et al. [9] have invented a new approach of reducing deposition within pMDI and has considered various parameters that have high impact on the deposition. It has been investigated that every patient using pMDIs have different technique of using the inhaler such as shaking procedure, actuating force applied onto the inhaler and inhalation airflow entering the mouth cavity as every patient has different breathing patterns. This in results

has impact on the amount of dosage entering the mouth cavity and then to lungs and also reduces the deposition performance. Therefore, an automated actuation system has been attached before the canister, which eject specific amount of droplets. Moreover, a sensor and actuator is attached at the exit duct of the inhaler. This consists of a cap on top of the exit, which when opens, gives a signal to the actuator to eject the droplets. Furthermore, a mixer consisting of blades is attached between the outlet duct and canister spray ejection region, which allows the droplets to get mixed with the air. The two ducts are also attached tangent to the mixer allows the ambient air to enter within the mixer. This process allows the droplets to get mixed with air and prepares enough dosage for the patient. As the mouth is attached, the dosage then enters the mouth cavity. This procedure reduces the impact of human abnormalities of using the pMDI and prevents from droplets deposition within the mouth cavity.

The present study has been carried out to investigate the droplets flow behavior within the VID at different velocity rates at the inlet. Ansys Fluent has been used to carry out numerical simulations to solve discrete phase model of salbutamol droplets with air. The second section comprises of numerical procedures and boundary conditions used in this study. Section 3 comprises the detailed investigations of flow patterns at different mass flow rates of air entering the VID. Section 4 concludes the results obtained for the VID.

2. Numerical Modelling of VID

The VID has been considered in the present study has been numerically modelled and analyzed to quantify the flow capacity of the inhaler. Detailed analyses of the complex flow behavior within the VID will be carried out.

2.1. Geometry and Spatial Discretization of the VID

The geometry of the VID is shown in figure 1(a). For realistic results, the geometry has been modelled as realistically as possible. It has been shown in many research studies [10-17] that the primary reason behind the differences between the numerical and experimental results is non-matching geometry. The CID consists of two inlet ducts, which are tangent to the inhaler body. Furthermore, particles from the canister enter to the inhaler body via small pipe. Additionally, the inhaler body is a mixer region, which acts as cyclone separator consisting three blades, causes suction within the inhaler body. This causes the airflow entering the inhaler body. The VID, containing the impeller blades, has been spatially discretized using tetrahedral elements. Tetrahedral elements offer higher numerical diffusion compared to hexahedral elements, which is another spatial discretization technique. Tetrahedral elements are preferred in complex geometries and in the regions where flow is non-uniform. Spatial discretization in the VID is shown in figure 1(b). A growth of 20% has been used from the first layer near the wall, indicating that the thickness of consecutive layers is 20% more compared to the previous layer.

2.2. Solver Settings

Specifications of appropriate boundary conditions are critical to the accuracy of any numerical analysis. In the present study, the inlet boundary of the flow domains has been specified as velocity inlets, while the outlet boundary has been specified as pressure outlet. The inlet velocity of 0.5m/s has been specified at each inlet duct of the VID. The outlet boundary condition of the flow domain has been specified with 0Pa gauge pressure. The walls of the flow domain (such as cyclone separator walls, inlet

duct walls, outlet duct walls etc.) have been modelled as no-slip boundaries, as expected in real-world. Furthermore, Salbutamol droplets have been ejected within the VID at 0.02seconds of the running time of impeller, to get it mixed with the air for 0.04seconds. The density of air and salbutamol is 1.225kg/m^3 and 1152kg/m^3 . The size of particles chosen is 0.0032mm , which are ejected inside the cyclone separator at the rate of 11.3m/s with the impeller rotational speed of 2000rpm . In order to resolve turbulence parameters numerically, Shear Stress Transport (SST) $k-\omega$ turbulence model has been used in the present study [18]. This turbulence model comprises of a cross-diffusion term in turbulent dissipation rate equation, along-with a blending function, to ensure that the model behaves appropriately in both near-wall and far-field zones. Reynolds Averages Navier-Stokes (RANS) equations [19-20], along-with the mass conservation and turbulence parameters' equations, have been iteratively solved for unsteady flow of air and Salbutamol particles within the VID. A convergence criterion of 0.001 for continuity, momentum conservation and turbulence parameters has been specified.

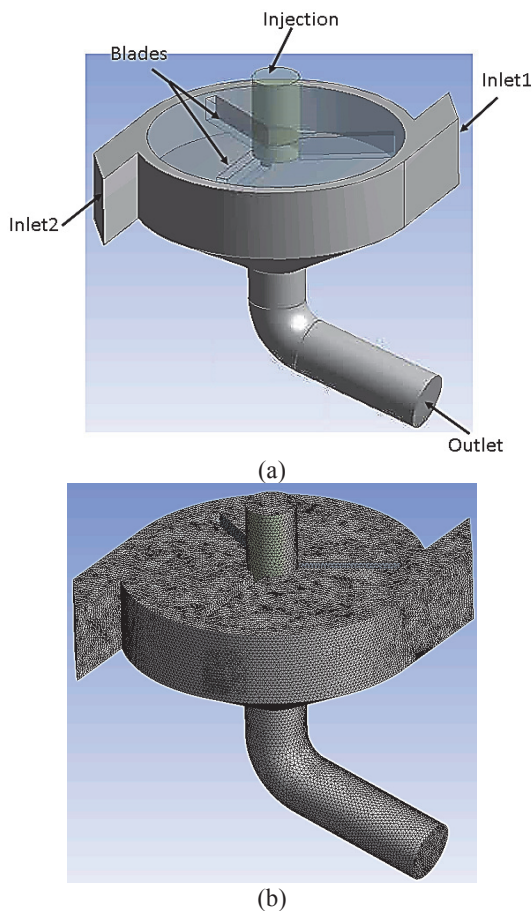


Figure 1. (a) Geometry of VID (b) Mesh within VID

3. Results and Discussions

The flow field within VID has been depicted in the form of pressure and velocity fields. Figure 2(a) depicts the static pressure variations within VID. It can be seen that the static pressure is higher within the cyclone separator and is lower at nose of the impeller and across the outlet duct. The static pressure is nearly 30Pa near the tips of the impeller region and reduced towards the impeller nose region and the center with a pressure drop of around 25Pa . This pressure drop is obtained as the cyclone separator has increased the angular momentum of the flow, which in-turn has increased the flow velocity. Increase of velocity magnitude reduces the static pressure within the cyclone separator.

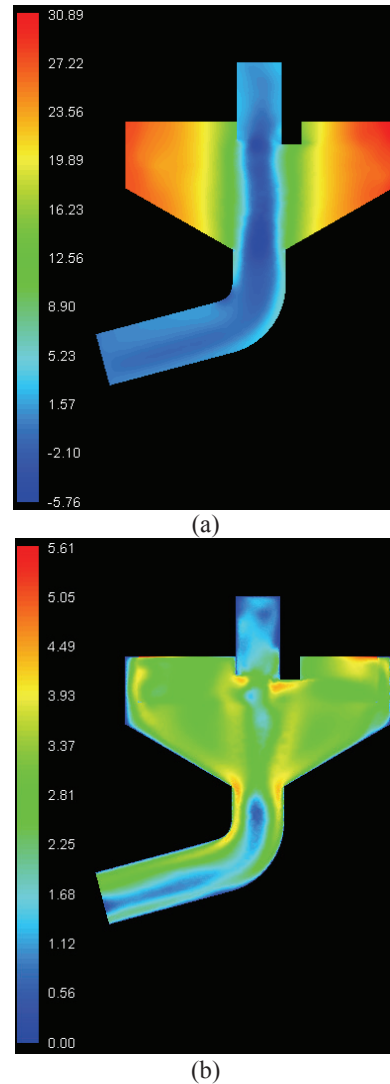


Figure 2. Flow variations within VID (a) Static pressure (Pa) and (b) Velocity magnitude (m/s)

Figure 2(b) depicts the velocity magnitude distribution within VID. It can be seen that the velocity magnitude is higher within the cyclone separator and is lower at nose of the impeller and across the outlet duct. The velocity magnitude is nearly 3.5m/s within the impeller passages and is higher near the blades due to rotational speed of impeller blades. The velocity magnitude is increased near the impeller tips region up to 5m/s . Furthermore, as the flow ejecting from the cyclone separator have a high vorticity, hence causing low velocity magnitude across the center and high radial velocity magnitude outwards.

3.1. Performance Analysis

To better understand the performance of VID, a systematic investigation has been carried out at various flow conditions, and at different rotational speeds. The aim here is to obtain the performance curves of VID. Design of Experiments (DoE) has been employed in the present study to determine the possible particle combinations of these parameters as shown in table 1. The inlet air velocity of 1m/s , 2m/s , 3m/s , 4m/s , 5m/s and 6m/s have been specified at each inlet duct [21] with the impeller speed of 1340rpm , 2100rpm and 2620rpm respectively for each design point as been carried out by Coates et al. The systematic investigation has also been carried out using the flow field within VID and has been depicted in the form of pressure and velocity fields.

Table 1. Factors and levels for full factorial design of diffuser configurations

Factors	Rotational speed (rpm)	Inlet velocity (m/s)
Level 1	1340	1
Level 2	2100	2
Level 3	2620	3
Level 4	-	4
Level 5	-	5
Level 6	-	6

Figure 3 depicts static pressure variations within VID at (a) inlet velocity of 1m/s (b) inlet velocity of 6m/s at rotational speed of 1340rpm respectively, and (c) inlet velocity of 1m/s at rotational speed of 2620rpm. It can be seen that the trend obtained within the inhaler body is similar to baseline geometry, having high static pressure near the impeller tip and the pressure drops in the center of the impeller region (impeller nose). Similarly, the pressure drops towards the outlet duct. However, as the inlet velocity is increased the static pressure is increased within the inhaler body as well. Furthermore, it also has been observed that by keeping the same velocity inlet of 1m/s but higher rotational speed of 2620rpm reduces the static pressure within inhaler body, however trend remains similar within the inhaler body.

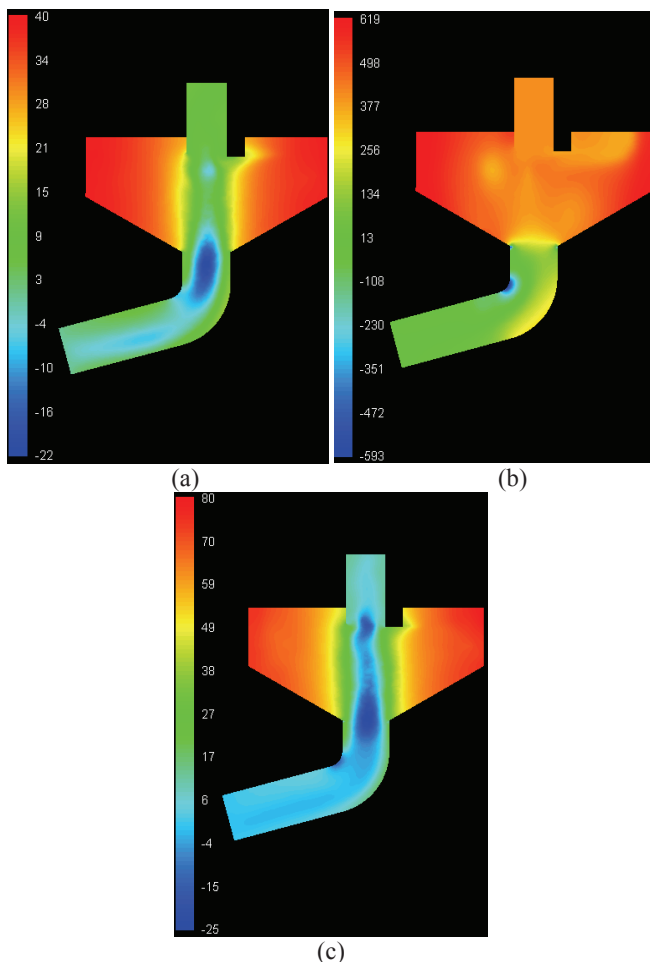


Figure 3. Static pressure (Pa) variations within VID at (a) inlet velocity of 1m/s (b) inlet velocity of 6m/s at rotational speed of 1340rpm respectively, and (c) inlet velocity of 1m/s at rotational speed of 2620rpm

A quantitative analysis has also been carried out whereby the pressure coefficient, C_p has been investigated at three different

design points at (a) inlet velocity of 1m/s (b) inlet velocity of 6m/s at rotational speed of 1340rpm respectively, and (c) inlet velocity of 1m/s at rotational speed of 2620rpm. It can be seen that pressure coefficient is higher when the inlet velocity is higher by keeping same rotational speed. Furthermore, the pressure coefficient drops as the rotational speed is increased by keeping the same inlet velocity. Moreover, it has also been observed that increasing inlet velocity reduces flow recirculation and angular velocity increase causes increase in flow recirculation, which could result in particle deposition on the inhaler body.

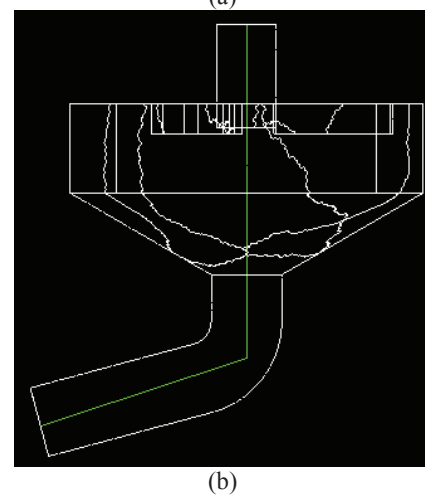
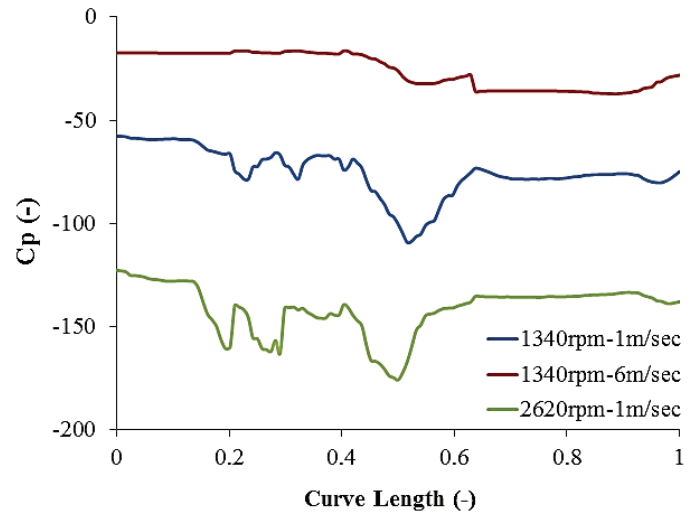


Figure 4. Pressure coefficient variations at three design points across the line shown in (b) of VID

Figure 5 depicts velocity magnitude distribution within VID at (a) inlet velocity of 1m/s (b) inlet velocity of 6m/s at rotational speed of 1340rpm respectively, and (c) inlet velocity of 1m/s at rotational speed of 2620rpm. It can be seen that the trend obtained within the inhaler body is similar to the baseline geometry, whereby the velocity magnitude is higher within the cyclone separator and is lower at nose of the impeller and across the outlet duct. Furthermore, as the inlet velocity increases at same rotational speed, the velocity magnitude rises within VID. However, the trend of the velocity magnitude remains similar. Moreover, it also has been observed that by keeping the same velocity inlet of 1m/s but higher rotational speed of 2620rpm increases the velocity magnitude within inhaler body; however, trend remains similar within the inhaler body.

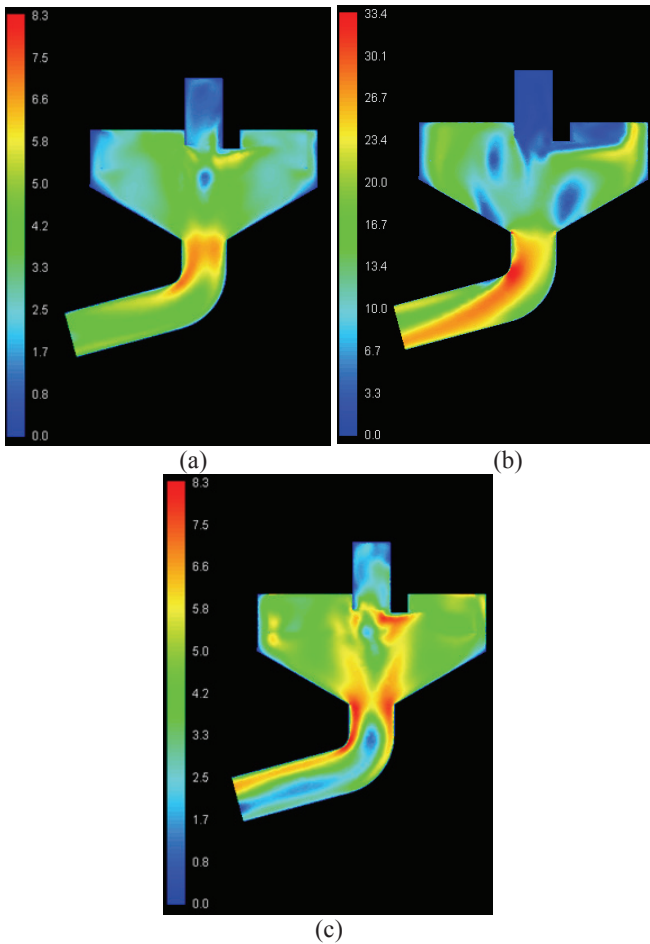


Figure 5. Velocity magnitude (m/s) distribution within VID at (a) inlet velocity of 1m/s (b) inlet velocity of 6m/s at rotational speed of 1340rpm (c) inlet velocity of 1m/s at rotational speed of 2620rpm

Figure 6 depicts Salbutamol particle dispersion rate (m/s) within VID at (a) inlet velocity of 1m/s (b) inlet velocity of 6m/s at rotational speed of 1340rpm respectively, and (c) inlet velocity of 1m/s at rotational speed of 2620rpm. It has been observed that increased inlet velocity causes particles velocity to increase with minimum flow recirculation, which results reduced particle deposition within inhaler body but could cause high dosage of Salbutamol on the mouth cavity. On the other hand, increased rotational velocity at with constant inlet velocity, increases the flow recirculation but has reduced flow rate of dosage. This result in high deposition rate within the inhaler body but does not have strong impact on the dosage.

4. Conclusions

A detailed investigation on flow variations and particle distribution has been conducted within VID. A full factorial based DoE has been employed in this study to understand the effect of variables considered on each other. It has been observed that increase of inlet velocity increases static pressure within the inhaler body and increase of rotational speed reduces the static pressure. Similarly, increase inlet velocity increases velocity magnitude within the inhaler body and increase of rotational speed also increases the velocity magnitude within VID. Moreover, it has been observed that increase of inlet velocity reduces the flow recirculation and projects all the flow towards the VID outlet. This results in reduced particle deposition within the inhaler body but increases the aerosol dosage. On the other hand, increased rotational speed increases the flow recirculation

and hence can cause the particle deposition. A detailed study needs to be carried out whereby an optimized sequence of inlet velocity and rotational speed has been selected where particle deposition is reduced. Furthermore, the effect of particle deposition rate has to be quantitatively investigated within the VID and its impact on the lungs.

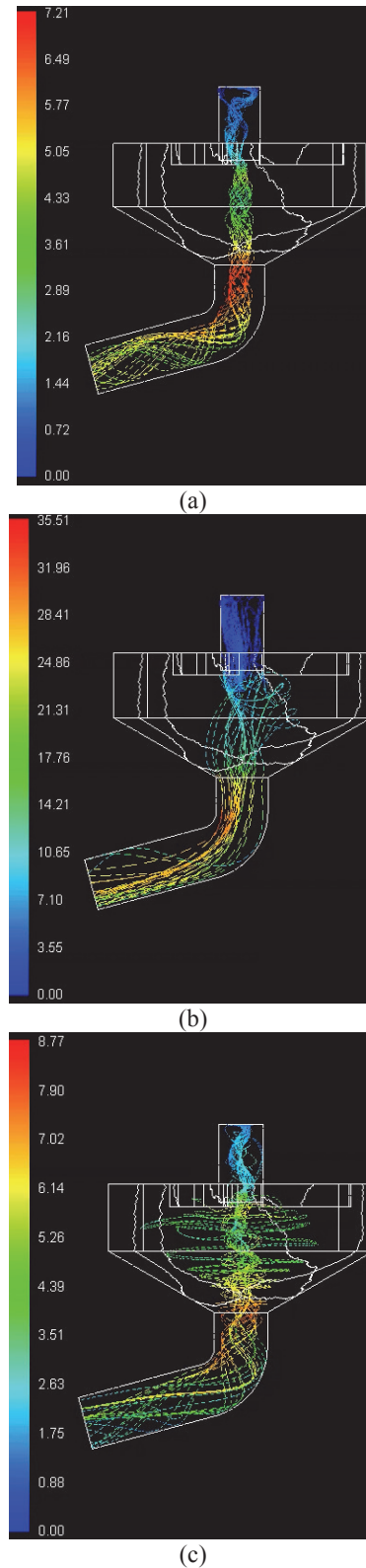


Figure 6. Salbutamol particle dispersion rate (m/s) within VID at (a) inlet velocity of 1m/s (b) inlet velocity of 6m/s at rotational speed of 1340rpm (c) inlet velocity of 1m/s at rotational speed of 2620rpm

References

- Dunbar, C.A. and Miller, J.F. (1997). Theoretical investigation of the spray from a pressurized metered-dose inhaler. *Atomization and Sprays*. Volume: 7.
- Dunbar, C.A., Watkins, A.P. and Miller, J.F. (1997). An experimental investigation of the spray issued from a pMDI using laser diagnostic techniques. *Journal of aerosol medicine*, Volume: 10. 351 – 368.
- Versteeg, H.K. Hargrave, G. Harrington, L. Shrubbs, I. and Hodson, D. (2000). The use of computational fluid dynamics (CFD) to predict pMDI air flows and aerosol plume formation. In *Respiratory Drug Delivery*. Volume: 7.
- Kleinstreuer, C. Shi, H. and Zhang, Z. (2007). Computational analyses of a pressurized metered dose inhaler and a new drug–aerosol targeting methodology. *Journal of aerosol medicine*. Volume: 20. 294 – 309.
- Leach, C.L. Davidson, P.J. and Boudreau, R.J. (1998). Improved airway targeting with the CFC-free HFA-beclomethasone metered-dose inhaler compared with CFC-beclomethasone. *European Respiratory Journal*. Volume: 12. 1346 – 1353.
- Cheng, Y.S. Fu, C.S. Yazzie, D. and Zhou, Y. (2001). Respiratory deposition patterns of salbutamol pMDI with CFC and HFA-134a formulations in a human airway replica. *Journal of aerosol medicine*. Volume: 14. 255 – 266.
- Leach, C.L. and Colice, G.L. (2010). A pilot study to assess lung deposition of HFA-beclomethasone and CFC-beclomethasone from a pressurized metered dose inhaler with and without add-on spacers and using varying breathhold times. *Journal of aerosol medicine and pulmonary drug delivery*. Volume: 23. 355 – 361.
- Oliveira, R.F. Teixeira, S.F. Silva, L.F. Teixeira, J.C. and Antunes, H. (2012). Development of new spacer device geometry: a CFD study (part I). *Computer methods in biomechanics and biomedical engineering*. Volume: 15. 825 – 833.
- Farina, S.H. Farina, D.J. and Pallas, S.R. (2017) Devices and methods for using medicament devices. Patent WO/2017/205824.
- Asim, T. Oliveira, A. Charlton, M. and Mishra, R. (2019). Improved Design of a Multi-Stage Continuous-Resistance Trim for minimum Energy Loss in Control Valves. *Energy*. Volume: 174. 954 – 971.
- Asim, T. Oliveira, A. Charlton, M. and Mishra, R. (2019). Effects of the Geometrical Features of Flow Paths on the Flow Capacity of a Control Valve Trim. *Petroleum science and Engineering*. Volume: 172. 124 – 138.
- Asim, T. Algadhi, A. and Mishra, R. (2018). Effect of Capsule Shape on Hydrodynamic Characteristics and Optimal Design of Hydraulic Capsule Pipelines. *Journal of Petroleum Science and Engineering*. Volume: 161. 390 – 408.
- Asim, T. Charlton, M. and Mishra, R. (2017). CFD based Investigations for the Design of Severe Service Control Valves used in Energy Systems. *Energy Conversion and Management*. Volume: 153. 288 – 303.
- Asim, T. and Mishra, R. (2017). Large Eddy Simulation based Analysis of Complex Flow Structures within the Volute of a Vaneless Centrifugal Pump. *Sadhana*. Volume: 42. 505 – 516.
- Asim, T. and Mishra, R. (2016). Optimal design of hydraulic capsule pipelines transporting spherical capsules. *Canadian Journal of Chemical Engineering*. Volume: 94. 966 – 979.
- Asim, T. and Mishra, R. (2016). Computational Fluid Dynamics based Optimal Design of Hydraulic Capsule Pipelines Transporting Cylindrical Capsules. *International Journal of Powder Technology*. Volume: 295. 180 – 201.
- Asim, T. Mishra, R. Abushaala, S. and Jain, A. (2016). Development of a Design Methodology for Hydraulic Pipelines Carrying Rectangular Capsules. *International Journal of Pressure Vessels and Piping*. Volume: 146. 111 – 128.
- Menter, F.R. (1994). Two-equation eddy-viscosity turbulence models for engineering applications. *AIAA*. Volume: 32. 1598 – 1605.
- Versteeg, H.K. and Malalasekera, W. (1995). *An Introduction to Computational Fluid Dynamics*. Longman Scientific and Technical, UK.
- Patankar, S.V. and Spalding, D.B. (2015). A calculation procedure for heat, mass and momentum transfer in three-dimensional. *Numerical Prediction of Flow, Heat Transfer, Turbulence and Combustion*. Volume: 54.
- Coates, M.S. Chan, H.K. Fletcher, D.F. and Raper, J.A. (2006). Effect of design on the performance of a dry powder inhaler using computational fluid dynamics. Part 2: air inlet size. *Journal of Pharmaceutical Sciences*. Volume: 95. 1382 – 1392.